NOAA TM ERL SEL-23

NOAA Technical Memorandum ERL SEL-23

U.S. DEPARTMENT OF COMMERCE
NATIONAL OCEANIC AND ATMOSPHERIC ADMINISTRATION
Environmental Research Laboratories

Observations of Proton Spectra ($1.0 \leq E_p \leq 300$ keV) and Fluxes at the Plasmapause

D.J. WILLIAMS
T.A. FRITZ
A. KONRADI

Space Environment Laboratory
BOULDER, COLORADO
February 1973

ENVIRONMENTAL RESEARCH LABORATORIES

SPACE ENVIRONMENT LABORATORY

IMPORTANT NOTICE

NATIONAL OCEANIC AND ATMOSPHERIC ADMINISTRATION

U.S. DEPARTMENT OF COMMERCE
National Oceanic and Atmospheric Administration
Environmental Research Laboratories

NOAA Technical Memorandum ERL SEL-23

OBSERVATIONS OF PROTON SPECTRA ($1.0 \leq E_p \leq 300$ keV) AND FLUXES AT THE PLASMAPAUSE

D. J. Williams
T. A. Fritz
Space Environment Laboratory

A. Konradi
Manned Spacecraft Center
National Aeronautics and Space Administration
Houston, Texas

Space Environment Laboratory
Boulder, Colorado
February 1973

U.S. DEPARTMENT OF COMMERCE
National Oceanic and Atmospheric Administration
ENVIRONMENTAL RESEARCH LABORATORIES
Boulder, Colorado 80302

Dear Colleague:

The attached NOAA Technical Memorandum ERL SEL-23, Observations of Proton Spectra ($1.0 \le E_p \le 300$ keV) and Fluxes at the Plasmapause, by D. J. Williams, T. A. Fritz, and A. Konradi is a revised version and supersedes an earlier Technical Memorandum ERL SEL-21, Observations of Proton Spectra ($1.0 \le E_p \le 300$ keV) and Pitch Angle Distributions at the Plasmapause, by D. J. Williams, T. A. Fritz, and A. Konradi.

This revision has been necessitated by the discovery of an engineering design flaw in the analog electronics associated with solid state proton detector aboard the S^3 satellite. This flaw has been discovered through many man months of very close analysis of in-flight data from the proton detector. The malfunction is caused by an amplifier in the analog amplifier chain becoming saturated due to excessive energy deposits in the solid state detector. The saturation condition extends the instrument dead time and under severe conditions causes a reduction in gain in the amplifier chain. Consequently in regions of intense high energy proton fluxes and/or alpha particle fluxes which are sharply peaked at equatorial pitch angles near 90° the low energy channels will show an intensity decrease as the detector swings through the region of equatorial 90° pitch angles. Our studies have shown several methods by which we can check to determine if this effect occurring and by which we can determine if the data is suspect or not. These are discussed briefly in the revised paper.

While the instability analysis discussed in the original paper remains valid, an unfortunate effect of the above condition is that we are unable to quantitatively establish an accurate pitch angle distribution as we enter the plasmapause during orbit 99. Very careful inspection of the data shows that butterfly pitch angle distributions; i.e., pitch angle distributions displaying minima at pitch angles of 90° apparently still do exist as the plasmapause is approached; however in orbit 99 the saturation effect does confuse the analysis and the distributions shown earlier having ratios of $j\ (\alpha = 35^\circ)/j\ (\alpha = 90^\circ) = (50\text{-}100)/1$, should in reality be $j\ (\alpha = 35^\circ)/j\ (\alpha = 90^\circ) = (2\text{-}3)/1$.

Several additional orbits have now been studied where the saturation condition can be eliminated as having any effects on the solid state proton detector data and confirm the above statement. These studies are now being finalized and a paper will be forthcoming in the future discussing details of these proton pitch angle distributions in the vicinity of the plasmapause.

Respectfully,

Donald J. Williams

Donald J. Williams, Director
Space Environment Laboratory

Attachment

OBSERVATIONS OF PROTON SPECTRA
($1.0 \leq E_p \leq 300$ keV) AND FLUXES
AT THE PLASMAPAUSE

D. J. Williams, T. A. Fritz, and A. Konradi*

Detailed proton spectral and pitch angle distribution observations have been obtained from instrumentation flown aboard the NASA Small Scientific Satellite, S^3-A (Explorer 45). S^3 was launched from Kenya, Africa, into an elliptical orbit having an apogee of 5.24 R_E, a perigee of 220 km, an inclination of 3.5^o, and a period of 7.82 hours. Data used in this initial report are from two proton detectors and a three-axis fluxgate magnetometer. Data from the magnetometer are used to routinely display the particle data as a function of local pitch angle. The lower energy proton instrument consists of an electrostatic analyzer-channeltron configuration measuring proton energies from 0.6 keV to 28 keV in sixteen energy intervals. The higher energy proton detector is a telescope detector system consisting of two surface-barrier solid-state detectors behind a 2.2 Kilogauss magnet used to sweep out electrons of energy less than 300 keV. Electrons of energy > 300 keV are detected via the coincidence mode of the telescope. This latter instrument measures protons from 24 keV to 300 keV in six intervals. The satellite spin axis was placed in the orbital plane, and all pitch angle distributions are obtained by sectoring the spin cycle into a number of samples.

*NASA Manned Spacecraft Center, Houston, Texas

For the data reported herein, thirty-two samples per spin period (8.451 seconds) were obtained. (See Longanecker and Hoffman, 1972, for a more detailed description of the satellite and instrumentation.)

Data from the solid state proton detector discussed earlier show an amplifier saturation effect in the presence of high energy ($\geq$ 1 Mev) protons. This saturation results in an extended dead time coupled with a decrease in gain and causes an apparent lowered count rate in the lowest five energy channels. The effect is complicated by the critical high energy count rate being energy dependent. A detailed report describing this effect, where it occurs, and how the data are checked will be available in the near future.

In general the saturation effect occurs in the region $2.5 \leq L \leq 3.5$. Also, its nature is such that if the lowest energy channel of the solid state proton detector is unaffected then all channels may be considered unaffected. Consequently two quick checks exist to determine normal operation:

(1) the best check of normal operation is to compare the highest energy channeltron proton channel (22.3-30.2 keV) with the lowest energy solid state proton channel (24.3-35.1 keV). Similar behavior indicates normal operation.

(2) inspection of counting rates in the high energy proton channels will give an indication where the data are suspect.

Here the data of interest are from S^3 orbit 99 inbound occurring on December 17, 1971, some eight hours before the sudden commencement of a magnetic storm occurring on that date. The magnetic conditions at the time are shown in Cahill (1972) where moderate magnetic activity (30-40 γ) is present from apogee to $L \sim 3$ on orbit 99.

These data have been carefully screened and suspect regions excluded from analysis. In figure 1 we show overlapping channels from the channeltron and solid state detector proton instruments for all of orbit 99 to illustrate how regions of normal and suspect data may be determined. Note the excellent agreement of the two instruments up to 0548 hours

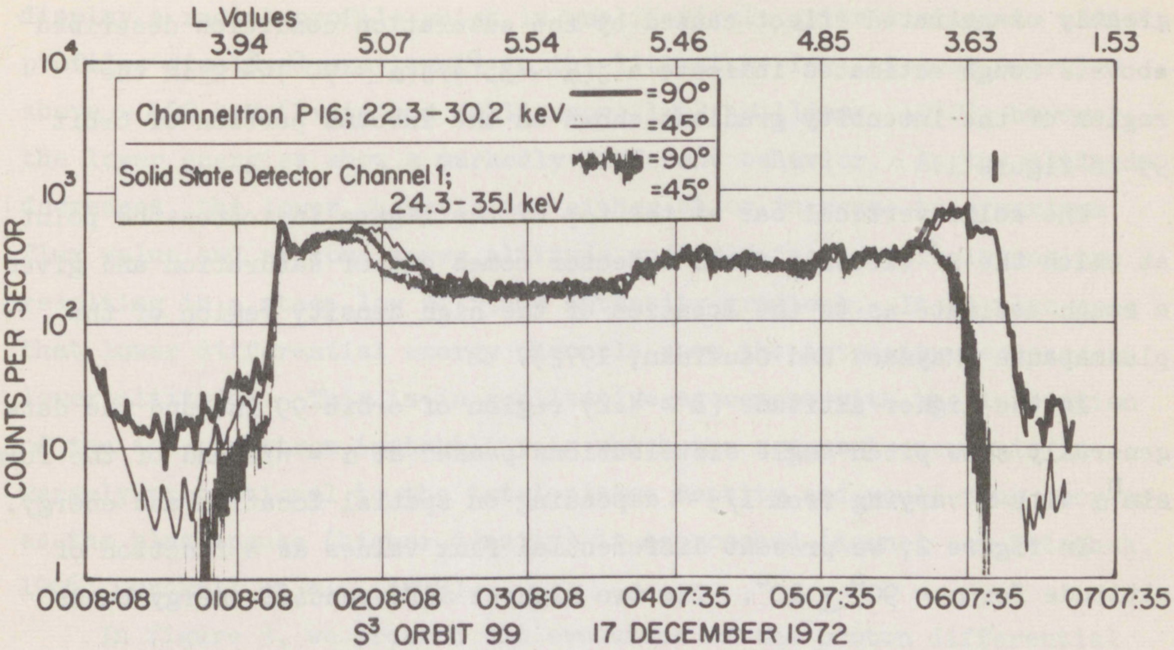

Figure 1. Proton intensities during S^3 orbit 99. Two energy channels (channeltron 22.3-30.2 keV and solid state detector 24.5-35.1 keV) each with two pitch angles ($\alpha = 90^\circ$ and 45°) are shown. Note excellent agreement throughout orbit up to 0548 hours where solid state detector channel departs significantly from channeltron channel. It is in this region where exaggerated "butterfly" pitch angle distributions are observed in lowest energy solid state detector channels due to amplifier saturation effects. Vertical bar at L = 3.45 (0614 hours) is where DC electric field comes out of saturation thereby providing indication of plasmapause (Maynard and Cauffman, 1972).

(including the "butterfly" pitch angle distributions shown near 0208 hours). At 0548 hours the solid state detector channel departs significantly from the channeltron data. It is in this region where we reported the development of pronounced "butterfly" pitch angle distributions having ratios $j(\alpha \sim 35^\circ)/j(\alpha \sim 90^\circ)$ of 50/1 to 100/1 (Williams et al., 1972). Careful inspection of both channeltron and solid state detector data in this region still indicates the development of an $\alpha = 90^\circ$ minimum in the pitch angle distribution, but the earlier data show a greatly exaggerated effect caused by the saturation condition described above. Rough estimates indicate a $j(\alpha \sim 35^{\circ})/j(\alpha \sim 90^{\circ}) \lesssim 2$ in the region of the intensity gradient shown on the inbound portion of orbit 99 in figure 1.

The solid vertical bar at the top of the figure indicates the point at which the S^3 electric field detector comes out of saturation and gives a rough estimate as to the location of the high density region of the plasmapause (Maynard and Cauffman, 1972).

In the higher altitude ($L \geq 4.2$) region of orbit 99 inbound the data generally show pitch angle distributions peaked at $\alpha = \pi/2$ and of the form $\sin^n \alpha$ with n varying from 1/3 - 4 depending on spatial location and energy.

In figure 2, we present differential flux values as a function of altitude for $\alpha = 90^{\circ} \pm 10^{\circ}$. The two highest differential energy bands

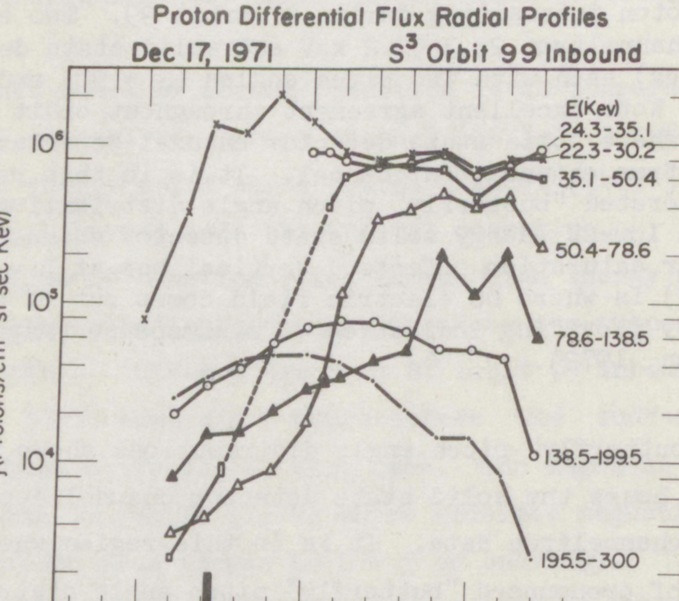

Figure 2. Proton differential flux versus altitude for six energy bands. Vertical bar at L = 3.45 same as in figure 1. Dashed line shows regions where data are not used.

display a radial profile which is qualitatively quite similar to radial profiles displayed previously in the literature for integral energies above ~ 100 keV (Davis and Williamson, 1963; Williams, 1970); however, the lower energies show a markedly different behavior. As the altitude decreases, the lower channels are either at or increase to a maximum flux value and at some lower altitude suddenly decrease in intensity resulting in a steep low altitude intensity gradient. It is also seen that lower differential energy channels show the intensity decrease at lower altitudes. This is in qualitative agreement with the initiation of the ion-cyclotron instability in which the resonant energy is inversely proportional to the total plasma density and would thus decrease as the plasmapause (higher density) is approached (Kennel and Petschek, 1966; Cornwall et al., 1970).

In figure 3, we present the evolution of the proton differential energy spectrum for $\alpha = 90^{\circ} \pm 10^{\circ}$ as the region of the spatial gradient is approached. Three points of interest in figure 3 are:

(1) the development of a deep trough in the differential energy spectrum.

(2) the appearance of a high energy peak in the differential energy spectrum.

(3) a build-up of intensities observed at energies just below the strongly resonant region indicative of significant energy diffusion especially at L = 3.6 and from 10-20 keV.

We present the following discussion arguing that the preceding data are consistent with the <u>initiation</u> of the ion-cyclotron instability that causes the initial decrease in intensities as the region of the radial gradient is approached.

Exponential wave growth is expected if the energetic proton population (see Kennel and Petschek, 1966; Cornwall et al., 1970) satisfies the following conditions:

$$A > \frac{1}{\frac{\Omega}{\omega} - 1} \qquad (1)$$

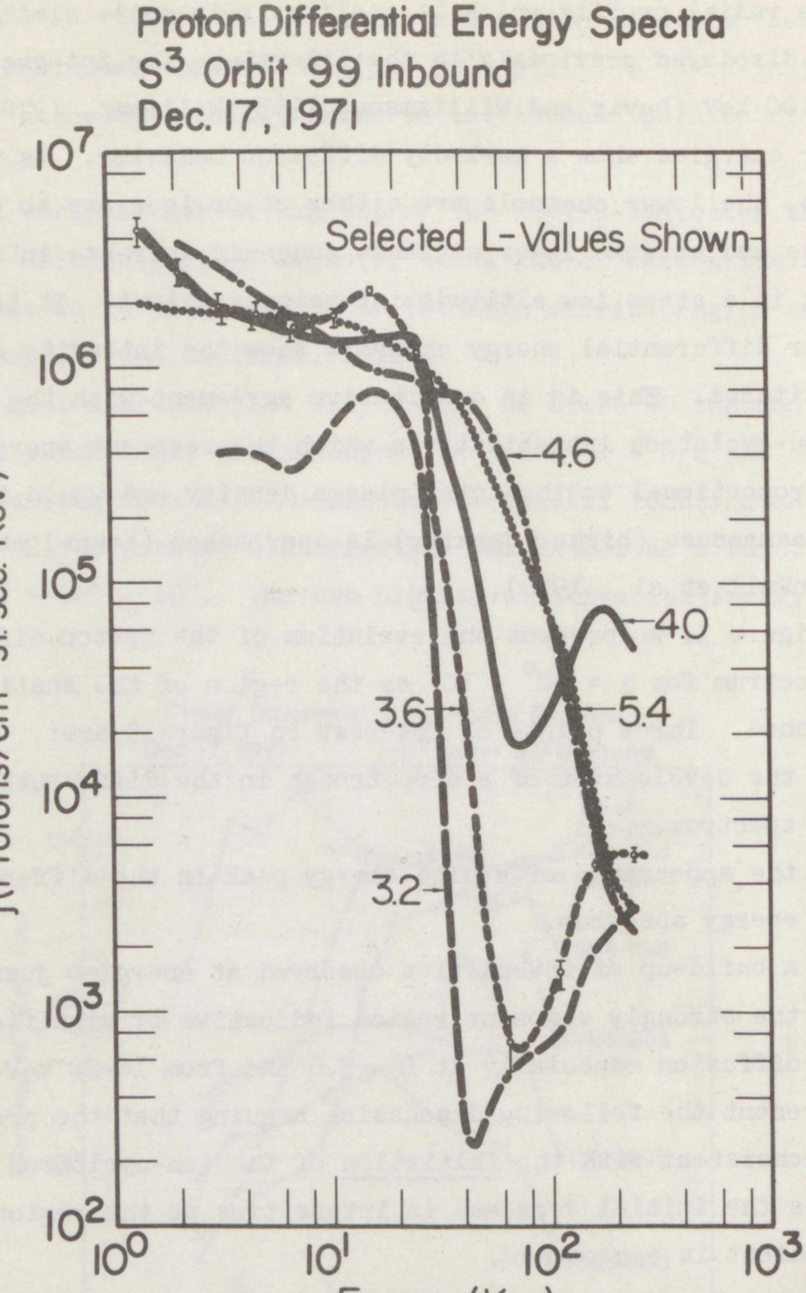

Figure 3. Evolution of proton differential energy spectra through region of steep gradient. No data available on L = 3.6 from 22 keV to 64 keV. No data available on L = 3.2 from 22 keV to 44 keV.

A = a measure of proton pitch angle anisotropy

($A \equiv n/2$ for $\sin^n\alpha$ distribution)

Ω = proton gyrofrequency

ω = wave frequency

$$J_{max}(E > E_R) > KL^{-4} \text{ protons/cm}^2\text{sec} \qquad (2)$$

L = McIlwain L parameter

E_R = parallel resonant energy

$$E_R > \frac{B^2}{8\pi N}\left(\frac{\Omega}{\omega}\right)^2\left(1 - \frac{\omega}{\Omega}\right)^3$$

or from (1) (3)

$$E_R > \frac{B^2}{8\pi N} A^{-2} (1 + A)^{-1}$$

B = magnetic field magnitude

N = total plasma density

Similar criteria hold for the stimulation of such instabilities in the energetic electron population (Kennel and Petschek, 1966) and the effects of the electron branch of the instability (whistler mode interaction) have been discussed in connection with electron precipitation phenomena (Brice, 1970; Brice and Lucas, 1971).

The pitch angle anisotropy identifies at a given point in space the wave frequencies that will resonate with the proton particle distribution. We thus interpret the <u>initiation</u> of the intensity decreases in figure 2 in the following manner. The lower differential channels show proton fluxes at high altitudes that exceed the limiting flux given in (2). As the altitude decreases, the resonant energy decreases because of an increasing plasma density as the plasmapause is approached. When the resonant energy matches a particular differential energy band, protons in that band suffer an intensity decrease caused by the initiation of the ion-cyclotron instability as all conditions are then met. As the altitude continues to decrease (N increasing) this effect is progressively seen through the lower energy channels displayed in figure 2. The high energy channels do not show similar effects because they do not exceed J_{max}.

To more quantitatively test this hypothesis, we show in figure 4 omnidirectional flux values versus altitude. Here we have summed through the lower energy channels which appear to be in resonance and have shown alone a higher energy channel which is apparently unaffected. For comparison, we have included a plot of the maximum allowed flux value from (2) for two values of the constant K, 5×10^{10} and $10^{10} cm^{-2} sec^{-1}$. From figure 4 we see that a critical flux value of $5 \times 10^{10} L^{-4}$ protons/cm^{2}sec

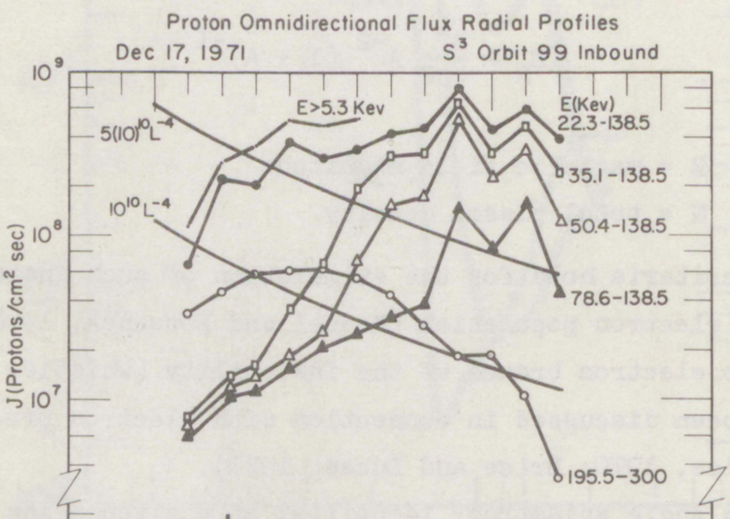

Figure 4. Omnidirectional fluxes versus altitude compared with $J_{max} = KL^{-4}$ for two values of K. Vertical bar at L = 3.45 same as in figure 1.

is consistent with earlier discussion. Theoretical estimates of K yield a lower limit of $5\text{-}7(10)^{10}\,cm^{-2}sec^{-1}$ (Kennel and Petschek, 1966; Cornwall, 1966) and recent low altitude experimental normalization of K has given $\sim 1.3(10)^{10}\,cm^{-2}sec^{-1}$ (Cornwall et al., 1971b).

Utilizing this interpretation we then are able to measure the resonant energy within a certain differential energy band as a function of altitude (see fig. 2) by obtaining the altitude at which the sudden intensity decrease occurs. We therefore can extract the total plasma density, N, as a function of altitude by observations of the resonant energy, E_R, the pitch angle anisotropy, A, and the magnetic field, B. This result is shown in figure 5. The vertical bars are the values of N extracted and reflect the fact that the resonant energy is measured as

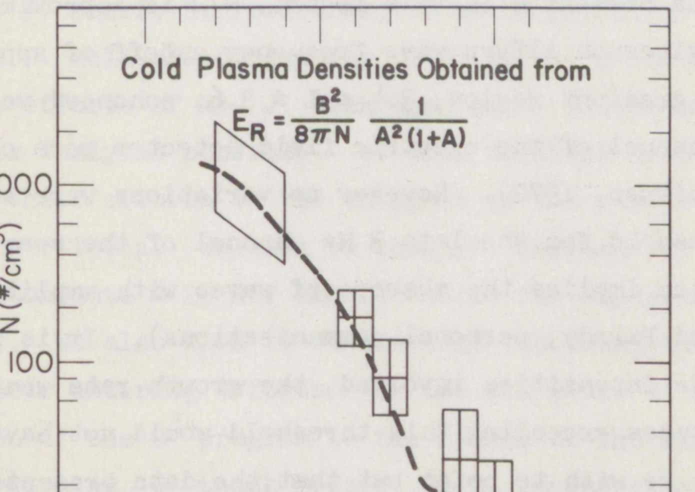

Figure 5. Plasma densities obtained from resonant energy equation with E_R, B, and A measured at or just before point of intensity decrease. N is extracted from equation shown in figure. Vertical range of N due to observation of E_R in particular energy interval. Dotted line simply indicates that a "normal" plasmapause is consistent with the data assuming initiation of ion-cyclotron resonance.

a differential energy band. A dashed line is drawn through the vertical bars to indicate that a normal plasmapause structure is obtained from the interpretation that the data in figures 2, 3, and 4 are consistent with the initiation of the ion-cyclotron instability.

If the above interpretation is correct and protons are put into strong pitch angle diffusion and are scattered into the atmosphere, the intensities shown in figures 2 and 3 should be sufficient to cause a mild red arc (Cornwall et al., 1971a). In checking the records of the Fritz Peak Observatory of the NOAA Aeronomy Laboratory, it was found that a mild red arc was observed at the time these observations were made (Hernandez, personal communication). Observations of the red arc occurred at near local midnight and the radial gradient displayed in figures 1 and 2 was observed as S^3 passed through the local midnight meridian.

For the data presented in this report, ω/Ω is approximately 1/5. At L = 4, this gives an Alfven wave frequency cutoff of approximately 1.6 Hz. In the gradient region, $3.4 \leq L \leq 3.6$, enhanced variations in the 1 to 4 Hz channel of the electric field detector were observed (Maynard and Cauffman, 1972). However no variations were seen above the sensitivity threshold for the 1 to 3 Hz channel of the search coil magnetometer which implies the absence of waves with amplitudes ≥ 0.1 gamma (Cahill and Parady, personal communications). It is possible that with the particle intensities involved, the growth rate would be such that wave amplitudes exceeding this threshold would not have occurred.

In summary, we wish to point out that the data presented here are consistent with the initiation of the ion-cyclotron instability when the requirements of equations (1), (2), and (3) are met. These requirements are met initially at the altitude at which the sudden intensity decrease occurs (fig. 3). However after the initiation of the instability, we find that the linear theory as outlined by (1), (2), and (3) does not explain the further evolution of the intensities and energy spectra of the ring current particles. First, the theory as it now stands has no mechanism whereby energy loss is formally introduced into the scattering mechanism. Second, the present theory also has no direct mechanism whereby the fluxes would precipitate much below J_{max}. Excluding parasitic precipitation effects (Lyons and Thorne, 1972), the instability should self-quench and basically return the particle fluxes to or just below J_{max}. However, we see from figures 2, 3, and 4 that this is not the case and the intensities continue to decrease to one to two orders of magnitude below this critical flux limit. Therefore, to describe the actual evolution of the data presented herein, we feel that non-linear effects, additional instabilities (e.g., see Coroniti et al., 1972), and particle injection and drift as a function of pitch angle (Konradi et al., 1972) must be considered in more detail.

ACKNOWLEDGMENTS

We wish to acknowledge valuable discussions with D. Evans, W. Bernstein, F. Scarf, R. Fredricks, J. M. Cornwall, G. Haerendel, N. Brice, and C. McIlwain concerning these data. It is a pleasure to recognize the efforts of Mr. J. Winkelman whose programming efforts have made this analysis possible. We wish to thank Drs. L. Lyons and H. Sauer for their efforts in the analysis of the causes and results of the saturation effects. We wish to thank R. Hoffman for discussions regarding proton data ≤ 25 keV and L. Cahill for magnetometer data used in this study. We also wish to acknowledge and thank the S^3 Project Office for their untiring efforts over the six years it required from the initiation of the S^3 program to the launch of the first spacecraft, S^3-A. In particular, we thank Messrs. G. W. Longanecker, F. Carr, K. Sizemore, R. A. Hoffman, and R. Martin. One of us (D.J.W.) wishes to thank NASA, GSFC, for the opportunity of having been associated with the inception, design, and development of the S^3 program and for having been allowed to serve as Project Scientist from November 1965 through August 1970. This work was done in part under NASA Contract S-50028.

REFERENCES

Brice, N. (1970), Artificial enhancement of energetic particle precipitation through cold plasma injection: A technique for seeding substorms?, J. Geophys. Res. 75: 4890.

Brice, N., and C. Lucas (1971), Influence of magnetospheric convection and polar wind on loss of electrons from the outer radiation belt, J. Geophys. Res. 76: 900.

Cahill, L. J., Jr. (1972), Magnetic storm inflation in the evening sector, Preprint, University of Minnesota, Minneapolis, Minn.

Cornwall, J. M. (1966), Micropulsations and the outer radiation zone, J. Geophys. Res. 71: 2185.

Cornwall, J. M., F. V. Coroniti, and R. M. Thorne (1970), Turbulent loss of ring current protons, J. Geophys. Res. 75: 4699.

Cornwall, J. M., F. V. Coroniti, and R. M. Thorne (1971a), Unified theory of SAR arc formation at the plasmapause, J. Geophys. Res. 76: 4428.

Cornwall, J. M., H. H. Hilton, and P. F. Mizera (1971b), Observations of precipitating protons in the energy range 2.5 keV $\leq$ E $\leq$ 200 keV, J. Geophys. Res. 76: 5520.

Coroniti, F. V., R. W. Fredricks, and R. White (1972), Instability of ring current protons beyond the plasmapause during injection events, Preprint, UCLA, to be published in J. Geophys. Res.

Davis, L. R., and J. M. Williamson (1963), Low energy trapped protons, Space Res. 3: 365.

Kennel, C. F., and H. E. Petschek (1966), Limit on stably trapped particle flux, J. Geophys. Res. 71: 1.

Konradi, A., D. J. Williams, and T. A. Fritz (1972), Energy spectra and pitch angle distributions of storm time and substorm injected protons, Preprint, NASA Manned Spacecraft Center, Houston, Tex.

Longanecker, G. W., and R. A. Hoffman (1972), S^3-A (Explorer 45) spacecraft and experiment description, Preprint, NASA Goddard Space Flight Center, Greenbelt, Md.

Lyons, L. R., and R. M. Thorne (1972), Parasitic pitch angle diffusion of radiation belt particles by ion-cyclotron waves, J. Geophys. Res. 77: 5608.

Maynard, N., and D. P. Cauffman (1972), Double floating probe measurements on S^3-A, Preprint, NASA Goddard Space Flight Center, Greenbelt, Md.

Williams, D. J. (1970), Trapped protons ≥ 100 keV and possible sources, in Particles and Fields in the Magnetosphere, pg. 396, B. M. McCormac, ed., D. Reidel Publishing Co., Dordrecht-Holland.

Williams, D. J., T. A. Fritz, and A. Konradi (1972), Observations of proton spectra ($1.0 \leq E_p \leq 300$ keV) and pitch angle distribution at the plasmapause, NOAA Tech. Memo, ERL-SEL-21, NOAA, Space Environment Laboratory, Boulder, Colo.